International Journal of Mechanical, Industrial and Aerospace Sciences
ISSN: 2517-9950
Vol:9, No:11, 2015

Lumped Parameter Models for Numerical Simulation of the Dynamic Response of Hoisting Appliances

Giovanni Incerti, Luigi Solazzi, Candida Petrogalli

Abstract—This paper describes three lumped parameters models for the study of the dynamic behavior of a boom crane. The models here proposed allows to evaluate the fluctuations of the load arising from the rope and structure elasticity and from the type of the motion command imposed by the winch. A calculation software was developed in order to determine the actual acceleration of the lifted mass and the dynamic overload during the lifting phase. Some application examples are presented, with the aim of showing the correlation between the magnitude of the stress and the type of the employed motion command.

Keywords—Crane, dynamic model, overloading condition, vibration.

I. Introduction

AS is known, the application of a load to a hoisting device generates vibrations due to the rope and structure elasticity [1], [2], [3], [4], [5]. This aspect is of a general nature and is independent from the type of structure and from the mode of application of the load; the dynamic effect, instead, is strongly influenced by these factors. For hoisting devices the phenomenon is particularly important as it generates dynamic actions whose wrong assessment, forgetfulness or omission could compromise the structure both as regards the maximum stress, the instability, the fatigue and the overall balance of the structure itself. Large literature on the subject has been prepared by many research groups [6], [7], [8], [9] as the problem, although overlooked at the design stage in the past, now plays a progressively more important role. In this paper, we deepens the study through the use of computational models with lumped parameters, that allow the designer to simulate the dynamic effects in function of the parameters of the hoisting system (mass, stiffness, natural frequencies, damping, etc.) and in functions of the motion law imposed by the winch to the load. These phenomena may be applied to other type of hosting machine like elevating work platform and it is independent of the material used to made the hoisting machine [10], [11]. The following paragraphs describe the mathematical models (with one or two degrees of freedom) and the resolution methods (analytical and numerical) of the motion equations generated by these models. Some practical examples of application of these models are finally shown, using as a reference a particular type of crane, which, depending on the position of the load and the lifting height, presents different dynamic behaviors as regards the stiffness of the structure and regards the stiffness of the rope.

G. Incerti, L. Solazzi and C. Petrogalli are with the Department of Mechanical and Industrial Engineering, University of Brescia, Via Branze 38, 25123 Brescia, Italy (e-mail: candida.petrogalli@unibs.it).

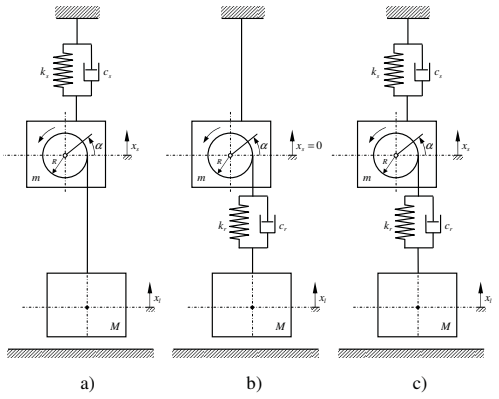

Fig. 1. Lumped parameter models of the crane

II. Dynamic models

To analyze the dynamics of a crane during the hoisting phase the designer can use one of the three models shown in Fig. 1. The choice of model depends on the stiffness of the components; in fact, if the stiffness of the ropes k_r is much higher than the stiffness of the structure k_s, the one degree of freedom (1 DOF) model in Fig. 1 (a) can be used; instead if the stiffness of the structure is large compared to the stiffness of the ropes, it is convenient to use the scheme in Fig. 1 (b), which considers the structure rigidly connected to the ground and the load elastically suspended. Finally, if both stiffnesses have the same order of magnitude, it is necessary to use the two degrees of freedom model (2 DOF) shown in Fig. 1 (c), where both the load and the structure are elastically suspended. In the following subsections these mathematical models are analyzed in detail, with particular reference to the deduction of the motion equations and to the solution techniques. A complete list of symbols used in Fig. 1 is shown in Table I.

A. One DOF model with rigid rope and elastic structure

For this type of model (Fig. 1 (a)) we use as free coordinate the displacement x_s of the structure; since the rotation α of the drum is known, the load displacement x_l is given by:

$$x_l = x_s + R\alpha \tag{1}$$

TABLE I
MODEL PARAMETERS

SYMBOL	DESCRIPTION
m	Mass of the structure
M	Mass of the load
k_s	Structural stiffness
c_s	Structural damping constant
k_r	Rope equivalent stiffness
c_r	Rope equivalent damping constant
R	Pulley radius

Using the Lagrangian approach, the system dynamics is described by the following equation:

$$\frac{d}{dt}\left(\frac{\partial T}{\partial \dot{x}_s}\right) - \frac{\partial T}{\partial x_s} + \frac{\partial \mathcal{R}}{\partial \dot{x}_s} + \frac{\partial \mathcal{V}}{\partial x_s} = 0 \tag{2}$$

where the symbols T, $\mathcal{V}$ ed $\mathcal{R}$ indicate respectively the kinetic energy, the potential energy (due to elastic deformation of the structure) and the Rayleigh dissipation function; for our problem these functions assume the form:

$$T = \frac{1}{2}(m\dot{x}_s^2 + M\dot{x}_l^2) = \frac{1}{2}[m\dot{x}_s^2 + M(\dot{x}_s + R\dot{\alpha})^2] \tag{3}$$

$$\mathcal{V} = \frac{1}{2}k_s x_s^2 \qquad \mathcal{R} = \frac{1}{2}c_s \dot{x}_s^2 \tag{4}$$

Substituting these expressions in (2) we obtain, after some mathematical manipulations, the motion equation of the system:

$$(m+M)\ddot{x}_s + c_s\dot{x}_s + k_s x_s = -MR\ddot{\alpha} \tag{5}$$

By defining $y = R\alpha$ this equation may be written as follows:

$$\ddot{x}_s + 2\xi_a\omega_a\dot{x}_s + \omega_a^2 x_s = -\lambda\ddot{y} \tag{6}$$

where:

$$\lambda = \frac{M}{m+M} = \frac{M}{m_t} \tag{7}$$

indicates the ratio between the load mass M and the total mass m_t of the system and the symbols:

$$\omega_a = \sqrt{\frac{k_s}{m_t}} \qquad \xi_a = \frac{c_s}{2\sqrt{k_s m_t}} \tag{8}$$

indicate, respectively, the natural frequency and the damping ratio of the system in Fig. 1 (a). If the hoisting acceleration $\ddot{y}$ is assigned as function of the time, (6) can be solved through the *convolution integral* that gives the solution $x_s(t)$ for null initial conditions; or the system under consideration, assuming that vibrations are underdamped ($\xi_a < 1$), this integral assumes the following expression [12]:

$$x_s(t) = -\frac{\lambda}{\omega_a^*}\int_0^t \ddot{y}(\tau)e^{-\xi_a\omega_a(t-\tau)}\sin[\omega_a^*(t-\tau)]d\tau \tag{9}$$

where:

$$\omega_a^* = \omega_a\sqrt{1-\xi_a^2} \tag{10}$$

indicates the damped natural frequency of the system. The integral can be calculated analytically in simple cases; for more complex cases, the evaluation of the integral can be performed using numerical techniques [13]. In the case where it is preferred to operate numerically it is appropriate to rewrite (6) in the form of a system of two first order differential equations: for this purpose, it is necessary first to make explicit the acceleration $\ddot{x}_s$ and to define two auxiliary functions:

$$u_1(t) = x_s(t) \qquad u_2(t) = \dot{x}_s(t) \tag{11}$$

which respectively represent the position and the velocity of the structure. From these definitions, we get immediately the following system:

$$\begin{cases} \dot{u}_1 = u_2 \\ \dot{u}_2 = -(\lambda\ddot{y} + 2\xi_a\omega_a u_2 + \omega_a^2 u_1) \end{cases} \tag{12}$$

whose solution can be obtained through a numerical integration procedure (Runge-Kutta, Wilson, etc.) [12] [13]. Currently these algorithms are implemented in the math libraries of many software applications for scientific calculations and therefore their use is simple and immediate.

B. One DOF model with elastic rope and rigid structure

To study the dynamics of the model shown in Fig. 1 (b) we use as free coordinate the load displacement x_l because the displacement x_s is identically zero, due to the infinite stiffness of the structure. Therefore the Lagrange equation takes the form:

$$\frac{d}{dt}\left(\frac{\partial T}{\partial \dot{x}_l}\right) - \frac{\partial T}{\partial x_l} + \frac{\partial \mathcal{R}}{\partial \dot{x}_l} + \frac{\partial \mathcal{V}}{\partial x_l} = 0 \tag{13}$$

where the kinetic energy, the elastic potential energy and the dissipation function are defined as follows

$$T = \frac{1}{2}M\dot{x}_l^2 \tag{14}$$

$$\mathcal{V} = \frac{1}{2}k_r(x_l - R\alpha)^2 \qquad \mathcal{R} = \frac{1}{2}c_r(\dot{x}_l - R\dot{\alpha})^2 \tag{15}$$

Substituting these expressions in (13) and calculating the respective derivatives, we obtain, with simple steps the motion equation of the system:

$$M\ddot{x}_l + c_r(\dot{x}_l - R\dot{\alpha}) + k_r(x_l - R\alpha) = 0 \tag{16}$$

Dividing by M all terms of (16), defining $y = R\alpha$ and introducing the relative coordinate $z = x_l - y$ (which expresses the difference between the load motion law and the motion law imposed by the winch), we get:

$$\ddot{z} + 2\xi_b\omega_b\dot{z} + \omega_b^2 z = -\ddot{y} \tag{17}$$

where:

$$\omega_b = \sqrt{\frac{k_r}{M}} \qquad \xi_b = \frac{c_r}{2\sqrt{k_r M}} \tag{18}$$

indicate respectively the natural frequency and the damping ratio of the system in Fig. 1 (b). Also in this case the solution can be easily obtained by means of the convolution integral; assuming $\xi_b < 1$ (underdamped system) and zero initial conditions, we have:

$$z(t) = -\frac{1}{\omega_b^*}\int_0^t \ddot{y}(\tau)e^{-\xi_b\omega_b(t-\tau)}\sin[\omega_b^*(t-\tau)]d\tau \tag{19}$$

where:

$$\omega_b^* = \omega_a\sqrt{1-\xi_b^2} \tag{20}$$

indicates the damped natural frequency of the system. After calculating the solution $z(t)$, the load displacement shifting x_l is easily calculated using the relation:

$$x_l(t) = z(t) + y(t) \tag{21}$$

If the equation is solved by numerical integration, it is necessary to operate as in the previous case, by rewriting the equation of motion in the form of a system of two first order differential equations;

By defining:

$$u_1(t) = z(t) \qquad u_2(t) = \dot{z}(t) \tag{22}$$

we obtain:

$$\begin{cases} \dot{u}_1 = u_2 \\ \dot{u}_2 = -(\ddot{y} + 2\xi_b\omega_b u_2 + \omega_b^2 u_1) \end{cases} \tag{23}$$

C. Two DOF model

For the study of the two degrees of freedom model in Fig. 1 (c) we use as independent coordinates x_l and x_s; the Lagrange equations of the system are:

$$\begin{cases} \dfrac{d}{dt}\left(\dfrac{\partial T}{\partial \dot{x}_l}\right) - \dfrac{\partial T}{\partial x_l} + \dfrac{\partial \mathcal{R}}{\partial \dot{x}_l} + \dfrac{\partial \mathcal{V}}{\partial x_l} = 0 \\ \dfrac{d}{dt}\left(\dfrac{\partial T}{\partial \dot{x}_l}\right) - \dfrac{\partial T}{\partial x_l} + \dfrac{\partial \mathcal{R}}{\partial \dot{x}_l} + \dfrac{\partial \mathcal{V}}{\partial x_l} = 0 \end{cases} \tag{24}$$

The kinetic energy, the elastic potential energy and dissipation function assume the following expressions:

$$T = \frac{1}{2}(M\dot{x}_l^2 + m\dot{x}_s^2) \tag{25}$$

$$\mathcal{V} = \frac{1}{2}[k_r(x_s + R\alpha - x_l)^2 + k_s x_s^2] \tag{26}$$

$$\mathcal{R} = \frac{1}{2}[c_r(\dot{x}_s + R\dot{\alpha} - \dot{x}_l)^2 + c_s\dot{x}_s^2] \tag{27}$$

Substituting these functions into Lagrange equations, the following system of differential equations is obtained:

$$\begin{cases} M\ddot{x}_l + c_r\dot{x}_l - c_r\dot{x}_s + k_r x_l - k_r x_s = f \\ m\ddot{x}_s - c_r\dot{x}_l + (c_r + c_s)\dot{x}_s - k_r x_l + (k_r + k_s)x_s = -f \end{cases} \tag{28}$$

where $f = R(k_r\alpha + c_r\dot{\alpha}) = k_r y + c_r\dot{y}$. Using the matrix notation we can rewrite this system in the form:

$$\mathbf{M}\ddot{\mathbf{x}} + \mathbf{C}\dot{\mathbf{x}} + \mathbf{K}\mathbf{x} = \mathbf{F} \tag{29}$$

where:

$$\mathbf{x} = \begin{Bmatrix} x_l \\ x_s \end{Bmatrix} \qquad \mathbf{F} = \begin{Bmatrix} f \\ -f \end{Bmatrix} \tag{30}$$

respectively indicate the displacement vector and the vector of forcing actions and

$$\begin{aligned} \mathbf{M} &= \begin{bmatrix} M & 0 \\ 0 & m \end{bmatrix} \\ \mathbf{C} &= \begin{bmatrix} c_r & -c_r \\ -c_r & (c_r + c_s) \end{bmatrix} \\ \mathbf{K} &= \begin{bmatrix} k_r & -k_r \\ -k_r & (k_r + k_s) \end{bmatrix} \end{aligned} \tag{31}$$

are respectively the mass, damping and stiffness matrices. The natural frequencies of the system can be calculated by solving the characteristic equation, which is obtained by setting equal to zero the determinant of the matrix $\mathbf{\Delta} = \mathbf{K} - \omega^2\mathbf{M}$; using symbolic algebra for this task and introducing the dimensionless ratios $\mu = M/m$ and $\kappa = k_r/k_s$ we have:

$$|\mathbf{\Delta}| = \omega^4 - A\omega^2 + B = 0 \tag{32}$$

where:

$$A = \frac{k_s}{m}\left(1 + \frac{\kappa}{\mu} + \kappa\right) \qquad B = \left(\frac{k_s}{m}\right)^2 \frac{\kappa}{\mu} \tag{33}$$

The positive solutions of (32) are the natural frequencies ω_1 and ω_2 of the hoisting system. The modal ratios γ_1 e γ_2 can be expressed in the form:

$$\begin{aligned} \gamma_i = \left(\frac{X_l}{X_s}\right)_{\omega=\omega_i} &= \frac{\kappa}{\kappa - \mu\omega_i^2\dfrac{m}{k_s}} \\ &= 1 + \frac{1}{\kappa}\left(1 - \omega_i^2\frac{m}{k_s}\right) \qquad i = 1, 2 \end{aligned} \tag{34}$$

where X_l and X_s are respectively the oscillation amplitudes of the load and the structure for the i^{th} normal mode of the system. Therefore the modal matrix $\mathbf{\Phi}$ can be written in the form:

$$\mathbf{\Phi} = [\mathbf{\Phi}_1\ \mathbf{\Phi}_2] = \begin{bmatrix} \gamma_1 & \gamma_2 \\ 1 & 1 \end{bmatrix} \tag{35}$$

Using this matrix it is possible to define the following relationship:

$$\mathbf{x} = \mathbf{\Phi}\mathbf{q} \tag{36}$$

that defines a linear transformation between the vector $\mathbf{x} = [x_l\ x_s]^T$ of the physical coordinates and the vector $\mathbf{q} = [q_1\ q_2]^T$ of the principal coordinates. As is known, the principal coordinates,do not have a physical meaning, but they allow to decouple the motion equations, transforming the system with two degrees of freedom in two independent systems with a single degree of freedom. Substituting (36) in (29) and pre-multiplying all terms by $\mathbf{\Phi}^T$ we get:

$$\mathbf{\Phi^T M \Phi}\ddot{\mathbf{q}} + \mathbf{\Phi^T C \Phi}\dot{\mathbf{q}} + \mathbf{\Phi^T K \Phi q} = \mathbf{\Phi^T F} \tag{37}$$

As is known, the property of orthogonality of the modal vectors with respect to the matrix and stiffness matrices allows you to write the following relationships:

$$\begin{aligned} \mathbf{\Phi}_i^T\mathbf{M}\mathbf{\Phi}_j &= 0 \qquad i \neq j \\ \mathbf{\Phi}_i^T\mathbf{M}\mathbf{\Phi}_i &= m_{ii}^* \quad i = 1, 2 \end{aligned} \tag{38}$$

$$\begin{aligned} \mathbf{\Phi}_i^T\mathbf{K}\mathbf{\Phi}_j &= 0 \qquad i \neq j \\ \mathbf{\Phi}_i^T\mathbf{K}\mathbf{\Phi}_i &= k_{ii}^* \quad i = 1, 2 \end{aligned} \tag{39}$$

Based on this property, it is possible then to write the following diagonal matrices:

$$\mathbf{M}^* = \mathbf{\Phi^T M \Phi} = \begin{bmatrix} m_{11}^* & 0 \\ 0 & m_{22}^* \end{bmatrix} \tag{40}$$

$$\mathbf{K}^* = \mathbf{\Phi^T K \Phi} = \begin{bmatrix} k_{11}^* & 0 \\ 0 & k_{22}^* \end{bmatrix} \tag{41}$$

Clearly, the natural frequenicies of the system can now be expressed in the form:

$$\omega_1 = \sqrt{\frac{k_{11}^*}{m_{11}^*}} \qquad \omega_2 = \sqrt{\frac{k_{22}^*}{m_{22}^*}} \tag{42}$$

Since the properties of orthogonality is not valid for the damping matrix, the matrix product $\mathbf{\Phi^T C \Phi}$ appearing in (37) does not generate a diagonal matrix and therefore the motion equations are coupled because of the damping terms. To solve this problem we introduce the hypothesis of proportional damping (or Rayleigh damping), according to which the damping matrix is expressed as linear combination of the mass and stiffness matrices; assuming known the coefficients a and b, we have:

$$\mathbf{C} = a\mathbf{M} + b\mathbf{K} \tag{43}$$

Substituting (43) in (37) and taking into account the (40) and (41) we obtain:

$$\mathbf{M}^*\ddot{\mathbf{q}} + [a\mathbf{M}^* + b\mathbf{K}^*]\dot{\mathbf{q}} + \mathbf{K}^*\mathbf{q} = \mathbf{Q} \tag{44}$$

where $\mathbf{Q} = \mathbf{\Phi^T F}$.

Clearly the matrix:

$$\mathbf{C}^* = a\mathbf{M}^* + b\mathbf{K}^* \tag{45}$$

is diagonal since it is calculated as a linear combination of two diagonal matrices. Substituting (45) in (44) we obtain two decoupled motion equations:

$$\mathbf{M}^*\ddot{\mathbf{q}} + \mathbf{C}^*\dot{\mathbf{q}} + \mathbf{K}^*\mathbf{q} = \mathbf{Q} \tag{46}$$

By solving (46) you get the solution in principal coordinates; the physical coordinates can be easily obtained using the linear transformation (36). If the modal vectors are properly normalized, is possible to transform the matrix $\mathbf{M}^*$ into the identity matrix $\mathbf{I}$; this operation is carried out multiplying each vector modal $\mathbf{\Phi}_i$ by a coefficient η_i, which makes the element m_{ii}^* equal to unity; therefore we have:

$$m_{ii}^* = (\eta_i \mathbf{\Phi}_i^T)\mathbf{M}(\eta_i \mathbf{\Phi}_i) = 1 \tag{47}$$

from which:

$$\eta_i = \frac{1}{\sqrt{\mathbf{\Phi}_i^T \mathbf{M} \mathbf{\Phi}_i}} \qquad i = 1, 2 \tag{48}$$

If $m_{ii}^* = 1$, then, according to (42), $k_{ii}^* = \omega_i^2$; it follows that the matrix $\mathbf{K}^*$ is transformed into the diagonal matrix $\mathbf{W}$ which contains the square of the natural frequencies of the system:

$$\mathbf{W} = \begin{bmatrix} \omega_1^2 & 0 \\ 0 & \omega_2^2 \end{bmatrix} \tag{49}$$

From (45) and (46), setting $\mathbf{M}^* = \mathbf{I}$ and $\mathbf{K}^* = \mathbf{W}$ we have:

$$\ddot{\mathbf{q}} + (a\mathbf{I} + b\mathbf{W})\dot{\mathbf{q}} + \mathbf{W}\mathbf{q} = \mathbf{Q} \tag{50}$$

or, in scalar form:

$$\ddot{q}_i + (a + \omega_i^2 b)\dot{q}_i + \omega_i^2 q_i = Q_i \qquad i = 1, 2 \tag{51}$$

Now, if we define:

$$a + \omega_i^2 b = 2\xi_i \omega_i \tag{52}$$

it is possible to obtain immediately the modal damping ratios ξ_i of the system:

$$\xi_i = \frac{a + \omega_i^2 b}{2\omega_i} = \frac{1}{2}\left(\frac{a}{\omega_i} + b\omega_i\right) \qquad i = 1, 2 \tag{53}$$

Of course, even for the two degrees of freedom model is always possible to operate numerically, using a solver for systems of differential equations. In this case it is necessary to rewrite the second order differential equations as four first-order equations. Therefore we proceed by expliciting from (29) acceleration vector:

$$\ddot{\mathbf{x}} = \begin{Bmatrix} \ddot{x}_l \\ \ddot{x}_s \end{Bmatrix} = \mathbf{M^{-1}}(\mathbf{F} - \mathbf{C}\dot{\mathbf{x}} - \mathbf{K}\mathbf{x}) \tag{54}$$

In this way, the two functions are defined:

$$\begin{cases} \ddot{x}_l = \mathcal{F}_1(x_l, \dot{x}_l, x_s, \dot{x}_s, t) \\ \ddot{x}_s = \mathcal{F}_2(x_l, \dot{x}_l, x_s, \dot{x}_s, t) \end{cases} \tag{55}$$

which provide, respectively, the load and the structure accelerations as a function of the displacements, velocities and time.

Introducing now the auxiliary functions:

$$\begin{array}{ll} u_1(t) = x_l(t) & u_2(t) = \dot{x}_l(t) \\ u_3(t) = x_s(t) & u_4(t) = \dot{x}_s(t) \end{array} \tag{56}$$

the system of four first order differential equations assumes the following form:

$$\begin{cases} \dot{u}_1 = u_2 \\ \dot{u}_2 = \mathcal{F}_1(u_1, u_2, u_3, u_4, t) \\ \dot{u}_3 = u_4 \\ \dot{u}_4 = \mathcal{F}_2(u_1, u_2, u_3, u_4, t) \end{cases} \tag{57}$$

III. Numerical simulations

The models described in Section II have been used for the dynamic study of a gantry crane; the purpose of this analysis is to verify the mechanical behavior of the crane for a given configuration in terms of stiffness and for a given motion command, in relation with the maximum lifting speed and acceleration. The motion law represented in Fig. 2 was defined. The speed was chosen increasing linearly for a time interval t_a and then held constant. The choice of a gantry crane was dictated by the large spread of this type of port cranes and by the fact that the great variability of the operating conditions (position of the arm and lift height)

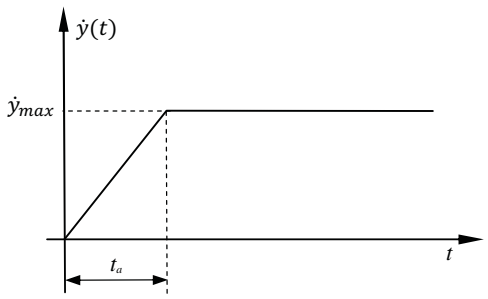

Fig. 2. Load velocity $\dot{y} = R\dot{\alpha}$ versus time

significantly affects the dynamic response of the machine. The first stage of the work has concerned the structural design of the crane; the performance characteristics of the machine and its dimensional parameters have been chosen so as to obtain a crane at the top of the category, with regard to size and load capacity. Specifically, we have adopted a maximum rated load of 50000 kg. Fig. 3 shows schematically the geometry of the machine. After a first dimensioning, carried out according to the commonly used standards for this type of crane (UNI EN 13001, DIN 15018), a three dimensional model, using SolidWorks software package, was prepared; subsequent finite element analysis (FEM) was performed using Simulation Multiphysics software by Autodesk. The crane structure has a stiffness in the vertical direction which depends on the position of the load on the arm (sea side or dock side). The stiffness value was determined through a FEM analysis.

In the position with the load on the sea side, i.e. during the picking phase of the container from the ship, the load application generates a bending of the arm tip of approximately 140 mm with respect to the reference position, corresponding to the configuration in which the crane is subjected only to the action of its own weight. Considering a load of 560 kN, the stiffness is equal to about 4000 N/mm. When the load is on the quay side, the deflection of the arm is approximately 35 mm compared to the static condition; therefore, always considering a load of 560 kN, the stiffness of the structure is approximately 16000 N/mm. The FEM analysis allowed to determine the first natural frequency of the structure and the equivalent modal mass; the first frequency is found to be equal to about 1.6 Hz and the modal mass of approximately 64000 kg, corresponding to 20% of the mass of the whole crane. The weights of the trolley, drums and accessories must be added to this value; on the basis of preliminary evaluations, the weight of these elements is equal to approximately 16000 kg and therefore the equivalent modal mass to be considered in the mathematical models is equal to 80000 kg. The rope stiffness depends on some parameters such as diameter, length and number of branches; adopting this variability, the rigidity of the rope ranges from 4000 N/mm in the case of lifting rope with 8 or 10 branches and diameter respectively 24 or 22 mm and from a height of 65 m to the maximum value of 30000 N /mm if instead the lifting height is reduced to 10 m. Fig. 4 and 5 show the crane deformation in different load conditions and in correspondence of the first natural frequency of vibration. For the assessment of the structure damping some tests similar to those present in literature [14], [15], [16] were conducted and a value equal to 5% for the structure and a value equal to 8% for the ropes were found. Fig. 6 show the results of some numerical simulations developed with the dynamic models described in section II. They refer to a maximum lifting speed of 100 m/min reached in 2 sec. This value is characteristic of high performance cranes commonly used in practice. Table II summarizes the parameters used for the simulations.

Fig. 4. Displacement of the crane with the pay load at sea side.

It was found a maximum acceleration of $1.6\,\mathrm{m/s^2}$ (Model B, Fig. 1) which corresponds to a load on the structure greater than 60% with respect to nominal one. This increase

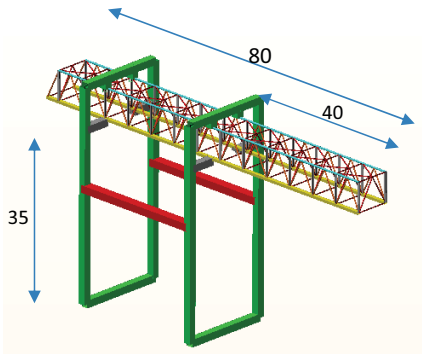

Fig. 3. Main dimensions of the designed crane [m]

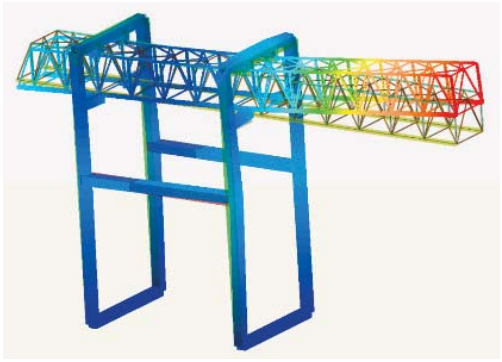

Fig. 5. Displacement of the crane in correspondence of the first mode of vibration (1.6 Hz).

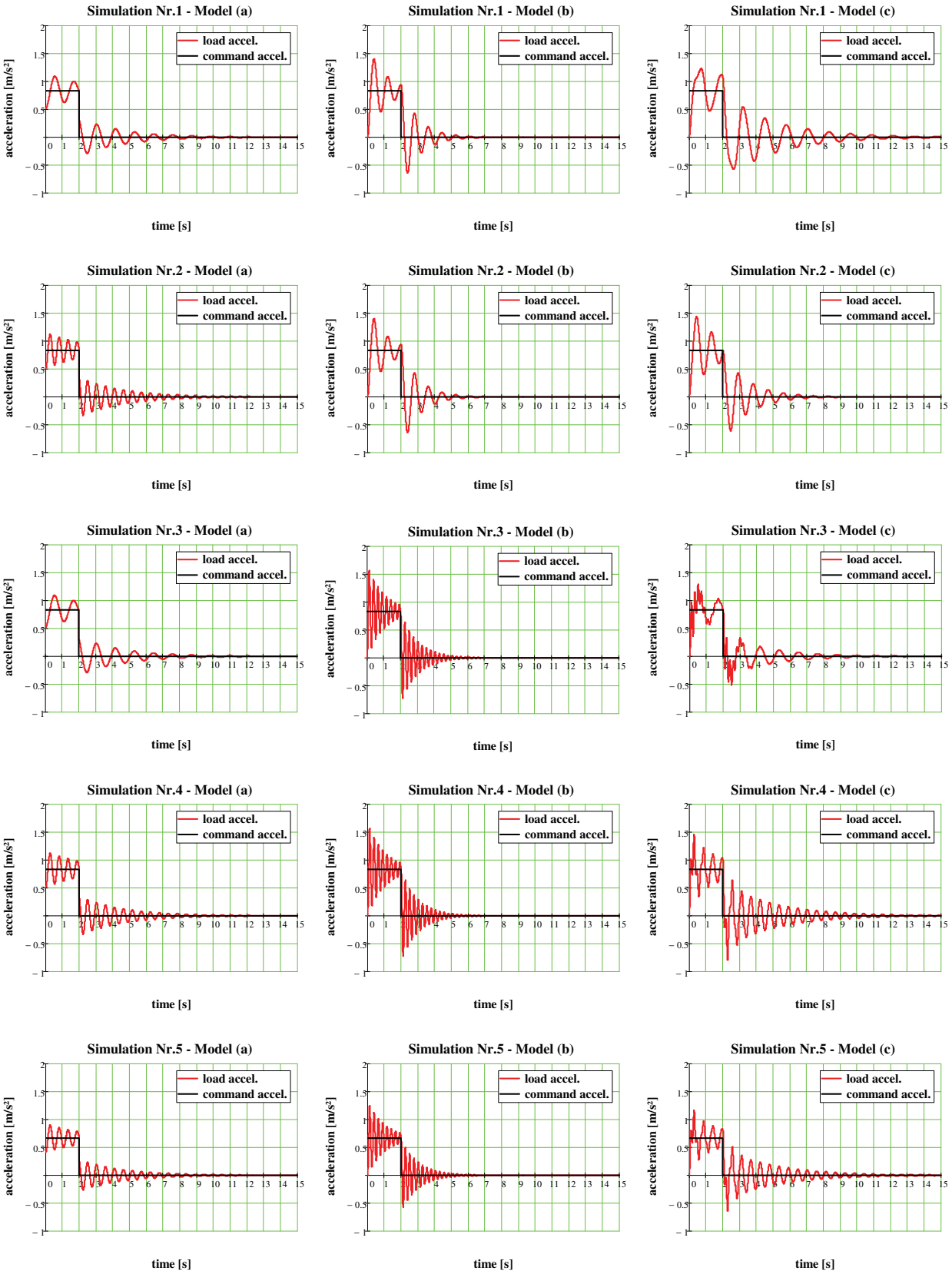

Fig. 6. Acceleration trend as a function of time in relation to the different configurations of the crane and the parameters of the law of motion

TABLE II
PARAMETERS USED FOR THE SIMULATIONS

Simulation Nr.	Model type	Mass of the structure	Mass of the load	Structural stiffness	Structural damping const.	Rope stiffness	Rope damping const.	Lifting speed	Accel. time	Max. load accel.	Min. load accel.
		m	M	k_s	c_s	k_r	c_r	v	t_a	a_{max}	a_{min}
		kg	kg	kN/m	Ns/m	kN/m	N/m	m/min	s	m/s²	m/s²
1	A	80000	50000	4000	100000	***	***	100	2	1,093	-0,287
	B	80000	50000	***	***	3000	100000	100	2	1,406	-0,643
	C	80000	50000	4000	100000	3000	100000	100	2	1,232	-0,573
2	A	80000	50000	18000	100000	***	***	100	2	1,123	-0,328
	B	80000	50000	***	***	3000	100000	100	2	1,406	-0,643
	C	80000	50000	18000	100000	3000	100000	100	2	1,438	-0,607
3	A	80000	50000	4000	100000	***	***	100	2	1,093	-0,287
	B	80000	50000	***	***	30000	100000	100	2	1,569	-0,719
	C	80000	50000	4000	100000	30000	100000	100	2	1,294	-0,507
4	A	80000	50000	18000	100000	***	***	100	2	1,123	-0,328
	B	80000	50000	***	***	30000	100000	100	2	1,569	-0,719
	C	80000	50000	18000	100000	30000	100000	100	2	1,452	-0,796
5	A	80000	50000	18000	100000	***	***	80	2	0,898	-0,262
	B	80000	50000	***	***	30000	100000	80	2	1,255	-0,575
	C	80000	50000	18000	100000	30000	100000	80	2	1,162	-0,637

of the load decreases significantly the safety coefficient of the structure. Since the typical design values for these cranes vary between 1.6 and 2, the precise determination of the maximum load acting on the structure becomes of fundamental importance. This fact on the one hand may cause exceeding in the yield point of the material of the crane and on the other may be responsible for local or global instability with consequent overturning of the structure. As known also in literature the maximum there is a relationship between the maximum acceleration value and the lifting speed [9].

Fig. 6 shows the result of a simulation with a lifting speed of 80 m/min. It can be clearly visible how the dynamic effect results reduced with respect to the simulation of Fig. 6 made with a lifting speed of 100 m/min. Even if only on a qualitative level it can be stated that the ratio between the maximum values of acceleration is correlated to the ratio between the lifting speed.

From the simulation it can be also observed that the number of load fluctuation results rather high and this can influenced the fatigue behavior of the structure (Fig. 6). Additionally also the amplitude of fluctuation cannot be neglected. Fig. 6 shows a decreasing in load amplitude from 1.2 to 0.4 the nominal value. The amplitude and the number of load fluctuation are related to many factors among which there are the stiffness and the damping of the structure and the rope. In this work these values were derived from literature or calculated through analitycal and numerical analyses (see Section II). Regarding these considerations, from the comparison between the models it was found that, for the crane considered, the model A underestimated the dynamic effect while the models B and C gave results comparable and in some cases stackable (Fig. 6). the higher the ratio k_s/k_r the greater the convergence of the results of the models B and C that, for values greater than 4 differed by only 5%. Finally, it can be concluded that to estimate the maximum acceleration experienced by the structure object of this application the scheme B is equally suited to the most complex scheme C.

IV. Conclusions

The work presented three dynamic models allow to analyze the dynamic effects induced by the lifting of a load.

The models have been implemented into a software that can be used during the design of a hoisting device to evaluate the dynamic behavior of a crane in different operating conditions. Particular attention was devoted to the calculus of the maximum acceleration of the load, since the safety of the lifting device is significantly influenced by this parameter.

In order to show the usefulness of the developed software, the paper presented a detailed analysis of a gantry crane, designed in accordance with the current technical standards; the analysis allowed the evaluation of the acceleration acting on the load in relation to the parameters of the dynamic models.

From the results of the numerical simulations the designer of a hoisting device can evaluate the dynamic overload conditions with a fast and sufficiently accurate procedure and modify the structural design of the machine so as to meet the requirements of safety required by the standards.

References

[1] Augustaitis V.K., Gican, V., Jakstas A., Spruogis B., Turla V., "Research of lifting equipment dynamics", *Journal of Vibroengineering*, Vol. 16, Issue 4, 2014, pp. 2082-2088.
[2] Zhang H.Z., Sheng X.Y., "Dynamics simulation of large tower structure lifting process based on CABLE modeling", *Applied Mechanics and Materials*, Vol. 533, 2014, pp. 145-153.
[3] Hu S.C., Zou N.B., Ouyang S., Zhang, W.Y., "Simulation Analysis about Dynamic Characteristics of Crane's Jib System Based on the Lifting Loads", *Advanced Materials Research*, Vol. 910, 2014, pp. 304-307.
[4] Chen S.T., Sun Z.X., Li X.D., Wang H.L., "Dynamic characteristic analysis of girder hoisting machine structure based on linear stiffness ratio", *Journal of Railway Engineering Society*, Vol. 31, Issue 11, 1 November 2014, pp. 77-81 and 97.
[5] Westover L., Olearczyk J., Hermann U., Adeeb S., Mohamed Y., "Analysis of rigging assembly for lifting heavy industrial modules", *Canadian Journal of Civil Engineering*, Vol. 41, Issue 6, 30 April 2014, pp. 512-522.
[6] Zhao Y.F., Sha L., Zhu Y., "Dynamic simulation analysis of the crane hoisting process based on Adams", *Advanced Materials Research*, Vol. 940, 2014, pp. 132-135.
[7] Bogdevičius M., Vika A., "Investigation of the dynamics of an overhead crane lifting process in a vertical plane", *Transport*, Vol. 20, Issue 5, 2005, pp. 176-180.

[8] Bao J., Zhang P., Zhu C., "Modeling and control of longitudinal vibration on flexible hoisting systems with time-varying length", *Procedia Engineering*, Vol. 15, 2011, pp. 4521-4526.
[9] Matteazzi S., Minoia F., "Dynamical overloading of lifting applicances submitted to vertical movements: use of one degree of freedom oscillating systems, equivalent to two degree of freedom systems", *Int. J. Materials and Product Technology*, Vol. 30, 2007, pp. 141-171.
[10] Solazzi L., "Design of an elevating work platform considering both the first and the second order effects and the inertial ones", *2nd Int. Conf. on Material and Component Performance under variable Amplitude Loading*, Darmstadt, Germany, March 23-26/2009.
[11] Solazzi L., Scalmana, R., "New Design Concept for a Lifting Platform made of Composite Material", *Applied Composite Materials*, ISSN 0929-189X Appl Compos Mater DOI 10.1007/s10443-012-9287-2, Published online: 14 September 2012.
[12] Rao S.S., *Mechanical Vibrations* - 5th ed., Prentice Hall, 2011.
[13] Press W.H., Teukolsky S.A., Vetterling W.T., Flannery B.P., *Numerical Recipes in C*, Cambridge University Press, 1992.
[14] Singh B., Nanda B.K., "Damping mechanism in welded structures", *World Academy of Science, Engineering and Technology*, Vol. 68, August 2010, pp. 319-324.
[15] Abdel Raheem S.E., "Dynamic characteristics of hybrid tower of cable-stayed bridges", *Steel and Composite Structures*, Vol. 17, Issue 6, 1 December 2014, pp. 803-824.
[16] Zhang B. L., Han Q. L., Zhang X. M., Yu X., "Sliding mode control with mixed current and delayed states for offshore steel jacket platforms", *IEEE Transactions on Control Systems Technology*, Vol. 22, Issue 5, September 2014, Article number 6687235, pp. 1769-1783.

Giovanni Incerti graduated in Mechanical Engineering in 1990 at the University of Brescia, Italy. At the same university he received the Ph.D in Applied Mechanics in 1995. Actually he is associate professor at the University of Brescia and his teaching activity is related to the courses of Mechanical Vibrations, Applied Mechanics and Vibration Control. He is author of papers dealing with the dynamic analysis of cam systems, the mathematical modeling of devices for industrial automation, the mechanism design by optimization techniques and the study of robots and servomechanisms.

Luigi Solazzi was born in Montichiari, Italy and went to the University of Brescia, where he studied mechanical engineering and obtained his degree in 1994. He is obtained PhD in the 2003. He works in the Department of Mechanical and Industrial Engineering of Brescia University and works for Machine Design Group.

Candida Petrogalli was born in Leno, Italy and went to the University of Brescia, where she studied mechanical engineering and obtained her degree in 2006. She is a PhD Student in Technologies and Energetic Systems for Mechanical Industry at the Department of Mechanical and Industrial Engineering of Brescia University and works for Machine Design Group.